

1 **Effect of bipolar electrode material on the reclamation**
2 **of urban wastewater by an integrated**
3 **electrodisinfection/electrocoagulation process**

4 Javier Llanos*, Salvador Cotillas, Pablo Cañizares, Manuel A. Rodrigo

5 Chemical Engineering Department, University of Castilla-La Mancha, Edificio Enrique
6 Costa Novella. Campus Universitario s/n, 13005 Ciudad Real, Spain

7 **Abstract.**

8 This work presents an integrated electrodisinfection/electrocoagulation (ED-EC) process
9 for urban wastewater reuse that employs iron bipolar electrodes. Boron doped diamond
10 (BDD) was used as the anode and stainless steel (SS) as the cathode. A perforated iron
11 plate was introduced between the anode and cathode to function as a bipolar electrode.
12 This ED-EC combined cell makes it possible to conduct the simultaneous removal of
13 microbiological content and elimination of turbidity from urban wastewater. The results
14 show that current densities greater than or equal to 6.70 Am^{-2} enable complete
15 disinfection of the effluent and the removal of more than 90% of its initial turbidity.
16 Hypochlorite and chloramines formed during the ED-EC process were found to be the
17 main compounds responsible for the disinfection process. Furthermore, a cell
18 configuration of cathode (inlet)-anode (outlet) improves the process performance by
19 enhancing turbidity removal. Finally, the influence of the bipolar electrode material (iron
20 or aluminium) was assessed. The results indicate that the efficiency of the
21 electrodisinfection process depends mainly on the anodic material and is not influenced
22 by the material of the bipolar electrode. In contrast, the removal of turbidity is more
23 efficient when using iron as a bipolar electrode, especially at low current densities, due

24 to the formation of a passive layer on the aluminium that hinders the dissolution of the
25 bipolar electrode.

26

27 **Keywords:** BDD, iron bipolar electrode, electrodisinfection, electrocoagulation,
28 integrated process.

29 *Corresponding author e-mail: javier.llanos@uclm.es. Tel.: +34-926-29-53-00 Ext.
30 3508; fax: +34-926-29-52-56

31

32

33

34

35

36

37

38

39

40

41

42

43

44

45

46

47

48

49

50

51

52

53

54

55 **1. Introduction.**

56 In recent years, electrochemical engineering has experienced great advances due to the
57 development of new electrode materials. For this reason, electrochemical technologies
58 have been widely used in wastewater treatment processes such as the removal of nutrients
59 (Bektas et al., 2004; Lacasa et al., 2011; Tran et al., 2011; Zaleschi et al., 2013),
60 disinfection of wastewater effluents (Cano et al., 2011; Ghernaout et al., 2011; Cui et al.,
61 2013) and degradation of organic compounds (Martínez-Huitle and Brillas, 2009; Alves
62 et al., 2013).

63 The choice of an appropriate electrode material is a matter of major importance to ensure
64 the success of an electrochemical process. In the case of coagulation, a technology applied
65 in urban wastewater treatment and reclamation (Pouet and Grasmick, 1995; Rodrigo et
66 al., 2010), aluminium and iron are the most commonly used electrode materials (Farhadi
67 et al., 2012; Mohora et al., 2012; Dubrawski et al, 2013). For the treatment of various
68 target effluent types, the different behaviours of iron and aluminium electrodes have been
69 assessed in the electrocoagulation of textile waste (Kobyta et al., 2003; Zongo et al., 2009),
70 baker's yeast wastewaters (Kobyta et al, 2008) and leachate (Ilhan et al, 2008), among
71 others. The results obtained have proven that the efficiency of the electrode material is
72 directly dependent on the nature of the wastewater being treated. Specifically, iron
73 electrodes have proved more efficient for Chemical Oxygen Demand (COD) removal
74 during the treatment of textile wastewaters, whereas the use of aluminium electrodes had
75 led to higher elimination percentages in the treatment of leachate and baker's yeast
76 wastewaters.

77 Electrochemical disinfection has become a good alternative for the removal of
78 microbiological content in wastewater (Martínez-Huitle and Brillas, 2008; Ghernaout and
79 Ghernaout, 2010; Pérez et al, 2010). This process consists mainly of the elimination of

80 faecal coliforms present in water through two potential mechanisms: the
81 electroadsorption of *Escherichia coli* (*E. coli*) on the electrode surface (direct
82 disinfection) (Golub et al, 1987; Ninomiya et al, 2013) and the formation of disinfectant
83 species that attack and eliminate *E. coli* (indirect disinfection) (Schmalz et al, 2009;
84 Bergmann, 2010). Again, the selection of the appropriate anode material for the
85 electrodisinfection process can affect the nature of the oxidising species formed; the most
86 common anode materials are boron doped diamond (BDD) and dimensionally stable
87 anodes (DSA) (Jeong et al, 2009; Gusmao et al, 2010; Haaken et al, 2012).

88 In the context of wastewater regeneration by electrochemical processes, our research
89 group recently demonstrated the technical viability of a combined reactor for the
90 simultaneous disinfection and removal of turbidity in actual effluents from municipal
91 wastewater treatment facilities, WWTF (Cotillas et al, 2013). In that work, the combined
92 electrodisinfection/electrocoagulation cell proposed was equipped with aluminium
93 bipolar electrodes. This cell was able to completely remove the microbiological content
94 in urban wastewaters at low applied electric charges (0.008 Ah dm^{-3}) and low current
95 densities (6.65 A m^{-2}). In addition, this cell facilitated a decrease in the turbidity of
96 wastewater by the electrodisinfection of the aluminium bipolar electrode and the
97 subsequent formation of coagulant species. However, the applied electric charge required
98 to reduce the turbidity was found to be higher than that necessary to disinfect the urban
99 wastewaters.

100 One of the key elements of the cell, which strongly affects the removal of turbidity, is the
101 material of the bipolar electrode. For this reason, and with the aim of optimizing the
102 efficiency of the proposed cell, it is necessary to confront a detailed study of the influence
103 of the bipolar electrode material on the process performance. Likewise, the comparison

104 of the behaviour of both materials can provide valuable information for the treatment of
105 actual wastewater by combined electrochemical processes involving electrocoagulation.

106 Based on these results, the main aim of the present work was to study the influence of the
107 bipolar electrode material (iron or aluminium) on the performance of an integrated
108 electrodisinfection/electrocoagulation process for the regeneration of urban wastewater
109 from the WWTF of Ciudad Real (Spain). The effects of the current density and cell flow
110 path on the process performance were also studied using iron as a bipolar electrode
111 material.

112

113 **2. Material and methods.**

114 This section describes the analytical techniques, experimental setup and experimental
115 procedure for the electrodisinfection/electrocoagulation process.

116

117 **2.1 Analytical techniques.**

118 The total iron and aluminium concentration was measured off-line using an inductively
119 coupled plasma spectrometer (Liberty Sequential, Varian) (detection limit <1.5 ppb)
120 according to a previously published standard method (APHA-AWWA-WPCF, 1998)
121 (plasma emission spectroscopy). To evaluate the total metal concentration, samples were
122 diluted to 50:50 (v/v) using 4 N HNO₃ to ensure total solubility of the metal.

123 Turbidity was measured using a 115 Velp Scientifica turbidimeter (measuring accuracy:
124 ±2%) according to a standard method described in the literature (APHA-AWWA-WPCF,
125 1998). This measurement was carried out after sedimentation (30 min without agitation,

126 typical settle time in reclamation of wastewaters) and filtration (0.45 μm filter) of the
127 samples.

128 Nitrogen and chloride inorganic anions (NO_3^- , NO_2^- , Cl^- , ClO^- , ClO_2^- , ClO_3^- , ClO_4^-)
129 were measured by ion chromatography using a Shimadzu LC-20A equipped with a
130 Shodex IC I-524A column; mobile phase, 2.5 mM phthalic acid at pH 4.0; flow rate, 1.0
131 ml min^{-1} (concentration accuracy: $\pm 0.5\%$). The peak corresponding to hypochlorite
132 interferes with that of chloride; therefore, the determination of hypochlorite was carried
133 out by titration with 0.001 M As_2O_3 in 2.0 M NaOH (Wilpert, 1957; Freytag, 1959). This
134 method consists of a redox determination to selectively quantify the hypochlorite
135 concentration, specifically, it is based on the redox reaction between the hypochlorite and
136 arsenite. Hypochlorite is reduced to chloride by the continuous addition of arsenite
137 whereas this last one is oxidized to arsenate. The pretreatment of the samples consists of
138 the addition of 2 ml of 2.0 M NaOH in order to increase the pH.

139 The same ion chromatography equipment (Shodex IC YK-421 column; mobile phase, 5.0
140 mM tartaric, 1.0 mM dipicolinic acid and 24.3 mM boric acid; flow rate, 1.0 ml min^{-1})
141 was used to measure the nitrogen inorganic cation (NH_4^+). Inorganic chloramines were
142 measured following the DPD standard method described in the literature (APHA-
143 AWWA-WPCF, 1998).

144 The faecal coliforms from wastewaters were estimated using the most probable number
145 (MPN) technique (APHA-AWWA-WPCF, 1998) (confidence level: 95%).
146 Microorganism counts were carried out by the multiple-tube-fermentation technique (24
147 h of incubation at 44 $^\circ\text{C}$) using 5 tubes at each dilution (1:10, 1:100, and 1:1000).

148 The presence of trihalomethanes (THMs) was evaluated by gas chromatography
149 (detention limit < 0.2 ppb) using a SPB 10 column (30 m x 0.25 mm; macroporous

150 particles with 0.25 μm diameter). Injection volume was set to 1 μL . Chloroform was the
151 only trihalomethane that could be generated because chloride is the only halogen that was
152 detected in the target wastewater. The presence of adsorbable organically bound halogens
153 using BDD anodes has been quantified in literature when working at current densities
154 higher than 25 A m^{-2} (Schmalz et al., 2009; Haaken et al., 2012). Nevertheless, these
155 halogenated organic derivatives were not measured in the present work due to the low initial
156 average organic matter in the target effluents (TOC_0 : 25 mg dm^{-3} ; COD_0 : 30 mg dm^{-3})
157 and also to the low values of the current densities selected (1.90-9.38 A m^{-2}), which
158 according to previous works prevent the formation of organochlorinated species (Cano et
159 al., 2011; Cano et al., 2012).

160

161 **2.2 Experimental setup.**

162 The electrodisinfection/electrocoagulation process was carried out in a single-
163 compartment electrochemical cell. In brief, this cell was a filter-press type in which a
164 perforated iron plate (2 mm thickness) was placed between the anode and cathode. The
165 electrode gap between anode and cathode was 27 mm and between anode or cathode and
166 the perforated bipolar electrode was 12.5 mm. The internal volume of the electrolysis cell
167 was 150 mL. The Fe foil acted as a bipolar electrode; the face exposed to the anode
168 worked as a cathode, and vice versa. Thus, the side of the Fe foil that faced the cathode
169 dissolved, allowing the generation of Fe species for the electrocoagulation process. BDD
170 (Adamant Technologies, Switzerland) was used as the anode material, and stainless steel
171 (SS) (AISI 304) (Mervilab, Spain) was used for the cathode. Both electrodes (BDD and
172 SS) were circular, with a geometric area of 78.5 cm^2 . The wastewater was stored in a
173 glass tank, stirred by an overhead stainless steel perforated flat plate stirrer (squared, 49

174 cm² of area). The stirrer speed was low (100 rpm) in order to prevent floc breakage. The
175 amount of water treated was 4000 ml.

176 The system worked in total recirculation mode, with a peristaltic pump (JP Selecta
177 Percom N-M328) continuously recycling the target wastewater. The volumetric
178 recirculation flow was 50 dm³ h⁻¹ during the experiments. All tests were carried out in
179 discontinuous mode. At this mode of operation, the production of oxidant and disinfectant
180 species is cumulative and it is related to the total Q (A h dm⁻³) applied at a given moment.
181 Agitation ensured the homogeneity of the system. The power supply was a Delta
182 Elektronika ES030-10. The temperature of the system was kept constant (25°C) by a
183 thermostatised bath and a heat exchanger. The samples were collected in the glass tank
184 and the sample volume was 100 ml. The *E. coli* and chlorine compounds (free and
185 combined) were measured immediately. In this way, it is not necessary the addition of
186 reagents (e.g. Na₂S₂O₃) to stop the reaction between microorganisms and disinfectant
187 species and therefore, the experimental error of the measure is minimized.

188

189 **2.3. Target effluents.**

190 The WWTF treats the wastewater of an average-sized town (Ciudad Real, 75000 p.e.)
191 located in the centre of Spain. The influent is domestic wastewater without a significant
192 industrial contribution. In order to minimize the influence of the characteristics of the
193 target effluent, several tests were carried out with the same sample and the samples were
194 taken in several consecutive days with similar weather conditions.

195 The average chemical and biological composition characteristics of the samples used in
196 this work is shown in Table 1.

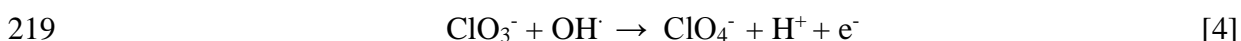
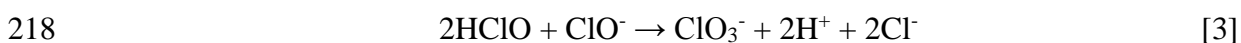
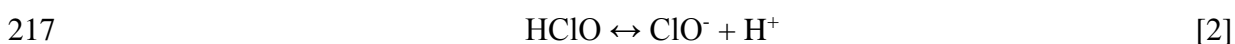
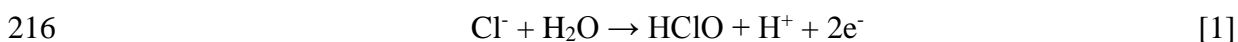
197 **3. Results and discussion.**

198 Within the present work, the influences of the current density, cell configuration and
199 bipolar electrode material on the process performance were evaluated.

200

201 **3.1. General behaviour of the ED-EC cell with Fe bipolar electrodes.**

202 Fig. 1.a shows the change in concentration of *E. coli* in an actual urban effluent during
203 the ED-EC process at an applied current density of 6.70 A m⁻². As can be observed, the
204 concentration of *E. coli* decreases with the applied electric charge following first-order
205 kinetics ($k = 0.3625 \text{ min}^{-1}$). This result can be related to several processes that occur
206 simultaneously in the electrochemical cell. As discussed in the introduction, the removal
207 of *E. coli* can take place on the anode surface by electroadsorption of microorganisms
208 (direct disinfection). However, the more advantageous electrode materials for this process
209 are fibrous carbon and graphite materials in the form of felt or cloth (Golub et al, 1987).
210 Microorganisms can also be removed by the generation of disinfectant species due to the
211 electrooxidation of ions naturally present in wastewater (indirect disinfection) (Schmalz
212 et al, 2009; Bergmann, 2010). One of the most common inorganic ions in municipal
213 treated wastewaters is chloride, which can be oxidised to hypochlorite, chlorate and
214 perchlorate according to Eqs. 1 to 4. The concentrations of these species (and
215 chloramines) are presented in Fig. 1.b.



220 Hypochlorite is the first chlorine compound formed by the electrooxidation of chloride
221 [Eq. 1-2]; it has been widely used in drinking water disinfection processes (Bergmann et

222 al, 2008). There is an initial increase in the hypochlorite concentration with the
223 application of the electric charge, followed by a decrease. The first trend observed is due
224 to the electrooxidation of chlorides present in wastewater, as mentioned previously. The
225 subsequent decline may be due to the elimination of *E. coli*, the oxidation of hypochlorite
226 to chlorates [Eq. 3] or the reaction of the electrogenerated hypochlorite with other
227 compounds such as ammonium to form chloramines [Eqs. 5-7].



231 As can be observed, the concentration of combined chlorine species increases with the
232 applied electric charge (Fig. 1.b), becoming the main disinfectant product at an applied
233 electric charge of 0.050 Ah dm⁻³. The presence of ammonium in the target effluent and
234 the consequent formation of chloramines is positive preferable due to the less reactive
235 and less aggressive nature of these compounds compared to hypochlorite. These
236 properties make the formation of organochlorinated species, which are harmful to human
237 health, less favourable (Lyon et al, 2012; Farré et al, 2013; Wang et al, 2013).

238 The pH did not vary appreciably during the test (average pH of 8.0) due to the undivided
239 nature of the proposed reactor and its resulting buffering behaviour. At this pH, the free
240 chlorine present in wastewater takes the form of hypochlorite ions, and the formation of
241 combined chlorine compounds is favoured (White, 1992; Mackay et al, 1999). Moreover,
242 because the pH is not altered, a subsequent neutralisation process (a step commonly
243 required in conventional coagulation processes) is not necessary.

244 The presence of chlorine compounds in high oxidation states has been detected,
245 specifically the formation of chlorates at high applied electric charges. Chlorates are

246 formed by the electrooxidation of hypochlorite, and their presence should be avoided in
247 wastewater because they are detrimental to human health. Regarding this point, it must
248 be highlighted that the evolution of chlorides to chloramines or chlorates and perchlorates
249 could be influenced by the initial composition of the target wastewater. In this context,
250 Pérez et al. (2012) reported the behaviour of chloride during the electrocatalytic treatment
251 of ammonium from synthetic solutions and landfill leachates using BDD anodes. They
252 concluded that a high initial chloride concentration (from 5,000 to 20,000 mg/L) favours
253 the production of free chlorine and the subsequent generation of inorganic chloramines
254 avoiding the formation of perchlorates, while a low initial concentration of chlorides
255 (lower than 2,000 mg/L) promotes the evolution of chlorides to chlorates and
256 perchlorates. Taking into account the low concentration of chloride of the target effluents
257 selected in the present work (around 200 mg/L), the presence of chlorate at certain current
258 densities is in accordance with the results previously presented in literature.

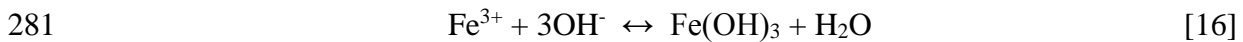
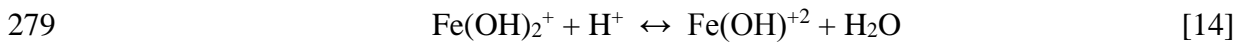
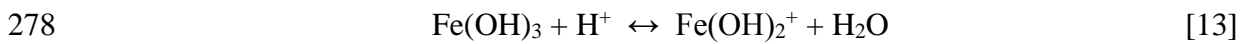
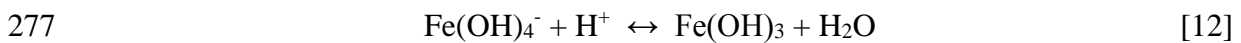
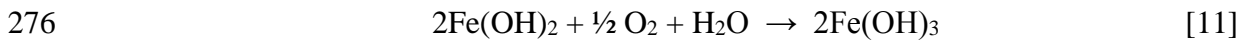
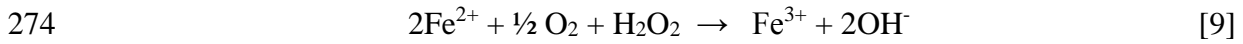
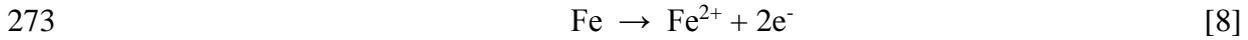
259 For this reason, the maximum applied electric charge allowed during the ED-EC process
260 is 0.020 Ah dm^{-3} . At this applied electric charge, disinfection is guaranteed, but the
261 production of chlorates is avoided.

262

263 Moreover, it is important to note that trihalomethanes, which could be formed due to the
264 reaction of hypochlorite with the soluble organic matter of the target wastewater (TOC_0 :
265 24 mg dm^{-3} ; COD_0 : 28 mg dm^{-3}), were not detected over the entire range of applied
266 electric charges in the test.

267 The second key parameter monitored throughout the test is turbidity. Fig. 2 shows the
268 evolution of this variable with the applied electric charge. The initial turbidity value is 14
269 NTU, and this parameter decreases with the applied electric charge, reaching a final value
270 of 1 NTU (93% turbidity removal). The observed behaviour is due to the generation of

271 soluble and insoluble coagulant species by the electrodisolution of the anodic side of the
272 bipolar iron electrode [Eqs. 8-16].



282 The total electrodisolved iron increases during the experiment, reaching a final value of
283 76.1 mg dm^{-3} . The nature of the iron species formed depends mainly on the pH and metal
284 concentration of the wastewater (Gregory and Duan, 2001; Duan and Gregory, 2003;
285 Cañizares et al, 2006; Cañizares et al, 2009). As discussed earlier in this manuscript, the
286 pH was naturally maintained at approximately 8 during the experiment. Thus, under these
287 operating conditions and according to the literature cited above, the dominant coagulant
288 species are insoluble hydroxide precipitates, and the mechanism of coagulation is sweep
289 flocculation.

290

291 **3.2. Influence of the key working variables on process performance.**

292 In this section, the influence of current density and flow path on the performance of the
293 cell was evaluated.

294

295 *3.2.1. Current density*

296 One of the most studied parameters in electrochemical processes is the current density
297 because this parameter can be directly related to the efficiency of reactions that occur on
298 the anode surface (Lacasa et al, 2012). Fig. 3 shows the changes in the *E. coli*
299 concentration during the ED-EC of urban wastewaters at different current densities.

300 As can be observed, the concentration of faecal coliforms decreases with the applied
301 electric charge, following first-order kinetics independent of the current density applied.
302 However, current densities equal to or greater than 6.70 Am^{-2} are required to achieve the
303 complete removal of *E. coli*. As previously demonstrated, the main compounds
304 responsible for the disinfection process are the disinfectant species electrogenerated
305 throughout the test. To shed light on the importance of the generation of these
306 electrogenerated species and the role that current density plays in their synthesis, Fig. 4
307 presents the concentration of free (Fig. 4.a) and combined (Fig. 4.b) chlorine species as a
308 function of the applied electric charge.

309 As can be observed, during the experiments conducted at 1.90 and 4.13 Am^{-2} , the
310 maximum concentrations of free and combined chlorine species were 0.005 , 0.010 mmol
311 Cl dm^{-3} (free) and 0.003 , $0.010 \text{ mmol Cl dm}^{-3}$ (combined), respectively. For a current
312 density of 6.70 Am^{-2} , the concentrations of both free and combined chlorine increased
313 dramatically, explaining the higher efficiency of the disinfection process at this current
314 density. In contrast, the maximum concentration of chlorine species detected at 9.38 Am^{-2}
315 is lower than that observed at 6.70 Am^{-2} . This result can be explained in terms of the
316 higher initial concentration of *E. coli* ($31,000$ vs. $22,000 \text{ CFU } 100 \text{ ml}^{-1}$) in the test carried
317 out at 9.38 Am^{-2} , which may result in a higher consumption of disinfectant and, thus, a
318 lower detected concentration.

319 With regard to the formation of chlorates and perchlorates, it was observed that the former
320 is detected when working at current densities from 6.70 Am^{-2} and charges higher than
321 0.020 Ah dm^{-3} . Perchlorate is not synthesised and the presence of trihalomethanes was
322 not detected at any of the current densities studied.

323 Fig. 5 shows the evolution of turbidity with the charge applied at increasing current
324 densities. As can be observed, the turbidity removal efficiency increases markedly with
325 current density until the applied current density reaches 6.70 Am^{-2} . This enhanced
326 performance is related to the higher efficiency of electrodisolution of the iron bipolar
327 electrode. Thus, the final total iron concentration that was electrodisolved increased from
328 4.96 to 76.1 mg dm^{-3} when the current density increased from 1.90 to 6.70 Am^{-2} . In
329 contrast, the trends observed during the experiments carried out at 6.70 and 9.38 Am^{-2} are
330 very similar, although it is possible to completely remove the turbidity of the target
331 effluent at the highest current density using an applied electric charge of 0.046 Ah dm^{-3} .

332 Finally, with respect to the change in pH, the behaviour observed for all current densities
333 studied is similar to that described in section 3.1; pH is naturally maintained at
334 approximately 8 due to the buffering effect of the undivided reactor.

335 In light of these results, it can be stated that the optimal current density for the proposed
336 EC-ED process with iron bipolar electrodes is 6.70 Am^{-2} . At this current density, it is
337 possible to conduct an efficient disinfection process together with significant removal of
338 turbidity. However, with the initial parameters of the treated effluent (*E. coli*₀: 22000
339 CFU 100ml⁻¹; turbidity₀: 14 NTU), the process is limited to a maximum applied electric
340 charge of 0.020 Ah dm^{-3} to avoid the generation of chlorates. At this value of electric
341 charge, the maximum removal of turbidity (close to 90%) is already reached, so this
342 restriction on the maximum allowable electric charge is not a constraint on the removal

343 of initial turbidity of the target effluent. This optimal current density could undergo
344 modifications if the initial composition of the target wastewater is drastically changed.

345 Finally, it is important to note that some authors (Yan et al., 1993; Kraft et al., 1999) have
346 reported the formation of calcareous deposits on the cathode surface during the treatment
347 of wastewaters containing Ca^{2+} and Mg^{2+} , due to the local increase in the pH that takes
348 place on the cathode (water reduction). However, this deposition of calcareous deposits
349 on the cathode surface was not observed in the present work. Moreover, the cell voltage
350 did not increase during the treatment, indicating that the properties of the cathode surface
351 were not modified. To explain this result, it is important to highlight that the calcium
352 concentration is lower than that reported by other researchers (Kraft et al., 1999).
353 Likewise, the low current densities used in the present work (maximum current density
354 of 9.38 A m^{-2} vs. 100 A m^{-2} of Kraft et al., 1999) reduce the formation of OH^- on the
355 cathode surface, preventing the formation of calcareous deposits.

356

357 3.2.2. Influence of the flow path.

358 In the first approach to the design of the combined EC-ED reactor using aluminium
359 bipolar electrodes (Cotillas et al, 2013), it was observed that the flow path played an
360 important role in the performance of the process. In the present work, the experiments
361 presented thus far were conducted with a cathode-anode (C-A) cell configuration: the
362 target wastewater enters the electrochemical reactor near the cathode and exits near the
363 anode (see Fig. SM-1 in the supplementary material). Fig. 6 shows the change in *E. coli*
364 concentration (Fig. 6.a) and turbidity (Fig. 6.b) with respect to the applied electric charge
365 at different cell configurations.

366 As can be observed, there were no significant differences in the disinfection efficiency of
367 the combined reactor when the flow path was changed. Thus, the microbiological content
368 decreased during the ED-EC process, achieving total removal of faecal coliforms at low
369 applied electric charges for both cell configurations.

370 Turbidity decreased with the applied electric charge, reaching a final value lower than 3
371 NTU in both cases (C-A: Final turbidity = 1 NTU; A-C: Final turbidity = 2 NTU).
372 However, the process was more efficient with a C-A cell configuration because of the
373 higher concentration of iron species formed (C-A: $76.1 \text{ mg Fe dm}^{-3}$; A-C: $55.5 \text{ mg Fe dm}^{-3}$).
374 This behaviour was previously described when using Al bipolar electrodes and can be
375 attributed to the improvement in mass transfer in the electrochemical cell when the
376 wastewater enters through the cathode side of the reactor and directly hits the anodic side
377 of the bipolar electrode. This event increases the turbulence inside the reactor (on the
378 anodic face) and favours the electrodisolution process.

379

380 **3.3. Influence of the bipolar electrode material on the ED-EC process.**

381 As previously mentioned, the main aim of the present work is to evaluate the effect of the
382 bipolar electrode material on the performance of the combined ED-EC cell. This
383 comparison between the results obtained with Al and Fe electrodes could be useful for
384 further optimisation of the combined process. Fig. 7 shows the percentage removal of *E.*
385 *coli* (Fig. 7.a) and turbidity (Fig. 7.b) using aluminium and iron bipolar electrodes at three
386 different applied electric charges and similar current densities.

387 As shown in Fig. 7.a, the *E. coli* are completely removed at low applied electric charges,
388 regardless of the material used for the bipolar electrode, with the differences in
389 elimination rate between the Al and Fe electrodes being negligible (iron: $k = 0.3625 \text{ min}^{-1}$

390 ¹; aluminium: $k = 0.3516 \text{ min}^{-1}$). The initially higher removal of *E. coli* by the iron
391 electrodes at a very low applied electric charge (0.001 Ah dm^{-3}) can be related to a slight
392 difference in the initial microbiological concentration of the effluent (iron: 22000 CFU
393 100 ml^{-1} ; aluminium: 24000 CFU 100 ml^{-1}). During the experiment with aluminium
394 bipolar electrodes, the maximum concentrations of free and combined chlorine species
395 were 0.055 and 0.015 mmol Cl dm^{-3} , respectively, while concentrations of 0.069 (free)
396 and 0.046 mmol Cl dm^{-3} (combined) were achieved with iron bipolar electrodes. The
397 differences observed in chlorine speciation, specifically in combined chlorine species, are
398 related to the initial concentration of ammonium in wastewater (aluminium: 23.095 mg
399 $\text{NH}_4^+ \text{ dm}^{-3}$; iron: 43.434 mg $\text{NH}_4^+ \text{ dm}^{-3}$). The higher initial ammonium concentration
400 enhances its reaction with the electrogenerated hypochlorite, resulting in a higher
401 concentration of chloramines in wastewaters when working with iron bipolar electrodes.
402 These results indicate that the disinfection process is mainly influenced by the anode
403 material of the electrochemical cell (BDD in both cases) rather than the material of the
404 bipolar electrode.

405 In contrast, the percentage of turbidity removal (Fig. 7.b) was strongly influenced by the
406 material of the bipolar electrode. The initial turbidity in wastewater was 8 NTU during
407 the process conducted with aluminium bipolar electrodes and 14 NTU when working with
408 iron electrodes. The elimination of turbidity during the experiment performed with iron
409 bipolar electrodes was higher when compared to aluminium electrodes. For example, at
410 the highest applied electric charge evaluated (0.050 Ah dm^{-3}), the use of iron electrodes
411 achieved an elimination of 92.86%, while aluminium electrodes removed 50%.

412 The superior turbidity removal with the use of iron electrodes can be explained by the
413 higher concentration of dissolved iron in comparison to aluminium, presented in Fig. 8.a.
414 Specifically, the total iron concentration achieved was $1.362 \text{ mmol Fe dm}^{-3}$ whereas 0.210

415 mmol Al dm⁻³ was obtained when working with aluminium electrodes at the same applied
416 electric charge (0.050 Ah dm⁻³).

417 The different efficiencies of Al and Fe dissolution in the ED-EC reactors can be explained
418 by passivation of the aluminium bipolar electrode under the conditions studied. It has
419 been well reported in the literature that aluminium can suffer from passivation due to the
420 formation of an Al₂O₃/Al(OH)₃ layer on the anode surface (Mechelhoff et al, 2013). This
421 passivation resulted in lower Al dissolution rates from the bipolar electrodes and
422 subsequently less efficient performance of the reactor in turbidity removal.

423 Theoretically, the presence of chloride, a well-known pitting promoter, should increase
424 the dissolution rate of the Al electrodes (Szkłarska-Smialowska, 1986). Nevertheless, to
425 promote the dissolution of the passive layer by the pitting effect of chlorides, it is
426 necessary to apply a potential greater than the so called pitting potential (Lee and Pyun,
427 2000). Thus, when working at low current densities (as in Fig. 7), the passivation of the
428 Al electrode dominated over the pitting effect of the chloride present in the target
429 wastewater. When a comparison of process performance was carried out at a higher
430 current density (and consequently at a higher applied potential), the efficiency of the
431 dissolution of the bipolar electrodes became similar (data presented in Fig. 8.b) due to the
432 breakage of the passive layer of the Al electrode.

433 Taking into account that disinfection can be efficiently conducted at low current densities
434 and low applied electric charges, the performance of the combined ED-EC process is
435 optimised when working with Fe bipolar electrodes, which avoid the formation of a
436 passive layer that would hinder the efficiency of the turbidity removal process.

437 Finally, the energy consumption per unit volume was calculated by means of the specific
438 electrical charge passed (Q, kAh m⁻³) and the average potential difference between anode
439 (BDD) and cathode (SS) [Eq. 17].

440
$$W \text{ (kWh m}^{-3}\text{)} = Q \cdot V \quad [17]$$

441 The energy consumption has been only calculated for the current densities in which the
442 *E. coli* has been completely removed (6.70 A m⁻² and 9.38 A m⁻²). The results show that
443 it is necessary 0.030 and 0.080 kWh m⁻³ to achieve the total disinfection of the effluent
444 for current densities of 6.70 A m⁻² and 9.38 A m⁻², respectively. The differences observed
445 in the required energy consumption can be related to the differences between the initial
446 concentrations of microorganisms in wastewater (j: 6.70 A m⁻², *E. coli*: 22000 CFU
447 100ml⁻¹; j: 9.38 A m⁻², *E. coli*: 31000 CFU 100ml⁻¹). However, the energy consumption
448 necessary to obtain a reclaimed water is lower than 0.1 kWh m⁻³ regardless the current
449 density applied and the initial characteristics of the wastewater.

450

451

452

453

454

455 **4. Conclusions.**

456 From this work, the following conclusions can be drawn:

- 457 - The integrated electrodisinfection/electrocoagulation process with BDD anodes
458 and perforated iron bipolar electrodes allows complete disinfection of the effluent
459 with simultaneously high percentages of turbidity removal.
- 460 - Hypochlorite and chloramines have been identified as the main compounds
461 responsible for the disinfection process. In addition, the presence of chlorates has

462 been detected for current densities greater than 6.70 Am^{-2} and applied electric
463 charges greater than 0.020 Ah dm^{-3} .

464 - A change in the flow path of the cell does not affect the efficiency of the
465 electrodisinfection process. Instead, a flow path from C-A enhances the
466 electrodissolution of the Fe foil and increases the rate of turbidity removal by
467 electrocoagulation.

468 - The bipolar electrode material does not significantly affect the efficiency of the
469 disinfection process. In contrast, Fe bipolar electrodes exhibit better performance
470 in the removal of turbidity at the low current density required to disinfect the target
471 effluent, which is due to the formation of a passive layer when Al is selected as
472 the bipolar electrode material.

473

474

475 **Acknowledgements**

476 The authors acknowledge funding support from the National Spanish Ministry of
477 Education and Science (Project CTM2010-18833) and Fundación Iberdrola through
478 grants for research on energy and environmental issues.

479 **References**

480

481 APHA-AWWA-WPCF, 1998. Standard Methods for the Examination of Water and
482 Wastewater, 17th ed. Clesceri, L.S., Greenberg, A. E., Eaton, A. D. 2108-2111.
483 Washington, DC.

484 APHA-AWWA-WPCF, 1998. Standard Methods for the Examination of Water and
485 Wastewater, 17th ed. Clesceri, L.S., Greenberg, A. E., Eaton, A. D. 3544-3551.
486 Washington, DC.

487 APHA-AWWA-WPCF, 1998. Standard Methods for the Examination of Water and
488 Wastewater, 17th ed. Clesceri, L.S., Greenberg, A. E., Eaton, A. D. 4563-4564.
489 Washington, DC.

490 APHA-AWWA-WPCF, 1998. Standard Methods for the Examination of Water and
491 Wastewater, 17th ed. Clesceri, L.S., Greenberg, A. E., Eaton, A. D. 9221-9227.
492 Washington, DC.

493 Alves, S.A., Ferreira, T.C.R., Migliorini, F.L., Baldan, M.R., Ferreira, N.G., Lanza,
494 M.R.V., 2013. Electrochemical degradation of the insecticide methyl parathion using a
495 boron-doped diamond film anode. *Journal of Electroanalytical Chemistry* 702, 1-7.

496 Bektas, N., Akbulut, H., Inan, H., Dimoglo, A., 2004. Removal of phosphate from
497 aqueous solutions by electro-coagulation. *Journal of Hazardous Materials* 106 (2-3), 101-
498 105.

499 Bergmann, H., 2010. A discussion on diamond electrodes for water disinfection
500 electrolysis. *GWF, Wasser - Abwasser* 151 (6), 604-613.

501 Bergmann, H., Koparal, A.T., Koparal, A.S., Ehrig, F., 2008. The influence of products
502 and by-products obtained by drinking water electrolysis on microorganisms,
503 *Microchemical Journal* 89 (2), 98-107.

504 Cano, A., Cañizares, P., Barrera, C., Sáez, C., Rodrigo, M.A., 2011. Use of low current
505 densities in electrolyses with conductive-diamond electrochemical — Oxidation to
506 disinfect treated wastewaters for reuse. *Electrochemistry Communications* 13 (11), 1268-
507 1270.

508 Cano, A., Cañizares, P., Barrera-Díaz, C., Sáez, C., Rodrigo, M.A., 2012. Use of
509 conductive-diamond electrochemical-oxidation for the disinfection of several actual
510 treated wastewaters. *Chemical Engineering Journal* 211-212, 463-469.

511 Cañizares, P., Martínez, F., Jiménez, C., Lobato, J., Rodrigo, M.A., 2006. Comparison of
512 the aluminum speciation in chemical and electrochemical dosing processes. *Industrial and*
513 *Engineering Chemistry Research* 45 (26), 8749-8756.

514 Cañizares, P., Jiménez, C., Martínez, F., Rodrigo, M.A., Sáez, C., 2009. The pH as a key
515 parameter in the choice between coagulation and electrocoagulation for the treatment of
516 wastewaters. *Journal of Hazardous Materials* 163 (1), 158-164.

517 Cotillas, S., Llanos, J., Cañizares, P., Mateo, S., Rodrigo, M.A., 2013. Optimization of an
518 integrated electrodisinfection/electrocoagulation process with Al bipolar electrodes for
519 urban wastewater reclamation. *Water Research* 47 (5), 1741-1750.

520 Cui, X., Quicksall, A.N., Blake, A.B., Talley, J.W., 2013. Electrochemical disinfection
521 of *Escherichia coli* in the presence and absence of primary sludge particulates. *Water*
522 *Research* 47 (13), 4383-4390.

523 Duan, J., Gregory, J., 2003. Coagulation by hydrolysing metal salts. *Advances in colloids*
524 *and interface science* 100-102, 475-502.

525 Dubrawski, K.L., Fauvel, M., Mohseni, M., 2013. Metal type and natural organic matter
526 source for direct filtration electrocoagulation of drinking water. *Journal of Hazardous*
527 *Materials* 244-245, 135-141.

528 Farhadi, S., Aminzadeh, B., Torabian, A., Khatibikamal, V., Alizadeh Fard, M., 2012.
529 Comparison of COD removal from pharmaceutical wastewater by electrocoagulation,
530 photoelectrocoagulation, peroxi-electrocoagulation and peroxi-photoelectrocoagulation
531 processes. *Journal of Hazardous Materials* 219-220, 35-42.

532 Farré, M.J., Day, S., Neale, P.A., Stalter, D., Tang, J.Y.M., Escher, B.I., 2013.
533 Bioanalytical and chemical assessment of the disinfection by-product formation potential:
534 Role of organic matter. *Water Research* 47 (14), 5409-5421.

535 Freytag, H., 1959. Zur Bestimmung von Hypochlorit, Chlorid und Chlorat in Chlorkalk.
536 *Fresenius' Zeitschrift für analytische Chemie* 171 (6), 458-458.

537 Ghernaout, D., Ghernaout, B., 2010. From chemical disinfection to electrodisinfection:
538 The obligatory itinerary?. *Desalination and Water Treatment* 16 (1-3), 156-175.

539 Ghernaout, D., Naceur, M.W., Aouabed, A., 2011. On the dependence of chlorine by-
540 products generated species formation of the electrode material and applied charge during
541 electrochemical water treatment. *Desalination* 270 (1-3), 9-22.

542 Golub, D., Ben-Hur, E., Oren, Y., Soffer, A., 1987. Electroadsorption of bacteria on
543 porous carbon and graphite electrodes. *Bioelectrochemistry and bioenergetics* 17 (2),
544 175-182.

545 Gregory, J., Duan, J., 2001. Hydrolyzing metal salts as coagulants. *Pure and Applied*
546 *Chemistry* 73 (12), 2017-2026.

547 Gusmão, I.C.C.P., Moraes, P.B., Bidoia, E.D., 2010. Studies on the electrochemical
548 disinfection of water containing escherichia coli using a dimensionally stable anode.
549 *Brazilian Archives of Biology and Technology* 53 (5), 1235-1244.

550 Haaken, D., Dittmar, T., Schmalz, V., Worch, E., 2012. Influence of operating conditions
551 and wastewater-specific parameters on the electrochemical bulk disinfection of
552 biologically treated sewage at boron-doped diamond (BDD) electrodes. *Desalination and*
553 *Water Treatment* 46 (1-3), 160-167.

554 Ilhan, F., Kurt, U., Apaydin, O., Gonullu, M.T., 2008. Treatment of leachate by
555 electrocoagulation using aluminium and iron electrodes. *Journal of Hazardous Materials*
556 154 (1-3), 381-389.

557 Jeong, J., Kim, C., Yoon, J., 2009. The effect of electrode material on the generation of
558 oxidants and microbial inactivation in the electrochemical disinfection processes. *Water*
559 *Research* 43 (4), 895-901.

560 Kobya, M., Delipinar, S., 2008. Treatment of the baker's yeast wastewater by
561 electrocoagulation. *Journal of Hazardous Materials* 154 (1-3), 1133-1140.

562 Kobya, M., Can, O.T., Bayramoglu, M., 2003. Treatment of textile wastewaters by
563 electrocoagulation using iron and aluminum electrodes. *Journal of Hazardous Materials*
564 *B* 100 (1-3), 163-178.

565 Kraft, A., Stadelmann, M., Blaschke, M., Kreysig, D., Sandt, B., Schröder, F., Rennau,
566 J., 1999. Electrochemical water disinfection. Part I: Hypochlorite production from very
567 dilute chloride solutions. *Journal of Applied Electrochemistry* 29 (7), 861-868.

568 Lacasa, E., Cañizares, P., Sáez, C., Fernández, F.J., Rodrigo, M.A., 2011.
569 Electrochemical phosphates removal using iron and aluminium electrodes. *Chemical*
570 *Engineering Journal* 172 (1), 137-143.

571 Lacasa, E., Llanos, J., Cañizares, P., Rodrigo, M.A., 2012. Electrochemical
572 denitrification with chlorides using DSA and BDD anodes. *Chemical Engineering*
573 *Journal* 184, 66-71.

574 Lee, W.-J., Pyun, S.-Y., 2000. Effects of sulphate ion additives on the pitting corrosion
575 of pure aluminium in 0.01 M NaCl solution. *Electrochimica Acta* 45 (12), 1901-1910.

576 Lyon, B. A., Dotson, A. D., Linden, K. G., Weinberg, H. S., 2012. The effect of inorganic
577 precursors on disinfection byproduct formation during UV-chlorine/chloramine drinking
578 water treatment. *Water Research* 46 (15), 4653-4664.

579 Mackay, D., MacLeod, M., Mattice, J., Solomon, K., 1999. Inorganic chloramines
580 (Priority substances list assessment report). Canadian Environmental Protection.

581 Martínez-Huitle, C.A., Brillas, E., 2008. Electrochemical alternatives for drinking water
582 disinfection. *Angewandte Chemie International Edition* 47 (11), 1998-2005.

583 Martínez-Huitle, C.A., Brillas, E., 2009. Decontamination of wastewaters containing
584 synthetic organic dyes by electrochemical methods: A general review. *Applied Catalysis*
585 *B: Environmental* 87 (3-4), 105-145.

586 Mechelhoff, M., Kelsall, G.H., Graham, N.J.D., 2013. Electrochemical behaviour of
587 aluminium in electrocoagulation processes. *Chemical Engineering Science* 95, 301-312.

588 Mohora, E., Rončević, S., Dalmacija, B., Agbaba, J., Watson, M., Karlović, E.,
589 Dalmacija, M., 2012. Removal of natural organic matter and arsenic from water by
590 electrocoagulation/flotation continuous flow reactor. *Journal of Hazardous Materials*
591 235-236, 257-264.

592 Ninomiya, K., Arakawa, M., Ogino, C., Shimizu, N., 2013. Inactivation of *Escherichia*
593 *coli* by sonoelectrocatalytic disinfection using TiO₂ as electrode. *Ultrasonics*
594 *Sonochemistry* 20 (2), 762-767.

595 Pérez, G., Gómez, P., Ibañez, R., Ortiz, I., Urriaga, A.M., 2010. Electrochemical
596 disinfection of secondary wastewater treatment plant (WWTP) effluent. *Water Science*
597 *and Technology* 62 (4), 892-897.

598 Pérez, G., Saiz, J., Ibañez, R., Urriaga, A.M. and Ortiz, I., 2012. Assessment of the
599 formation of inorganic oxidation by-products during the electrocatalytic treatment of
600 ammonium from landfill leachates. *Water Research* 46 (8), 2579-2590.

601 Pouet, M.-F., Grasmick, A., 1995. Urban wastewater treatment by electrocoagulation and
602 flotation. *Water Science and Technology* 31 (3-4), 275-283.

603 Rodrigo, M.A., Cañizares, P., Buitrón, C., Sáez, C., 2010. Electrochemical technologies
604 for the regeneration of urban wastewaters. *Electrochimica Acta* 55 (27), 8160-8164.

605 Schmalz, V., Dittmar, T., Haaken, D., Worch, E., 2009. Electrochemical disinfection of
606 biologically treated wastewater from small treatment systems by using boron-doped
607 diamond (BDD) electrodes - Contribution for direct reuse of domestic wastewater. *Water*
608 *Research* 43 (20), 5260-5266.

609 Szklarska-Smialowska, Z., 1986. Pitting Corrosion of Metals. National Association of
610 Corrosion Engineers, Houston, TX.

611 Tran, N., Drogui, P., Blais, J.-F., Mercier, G., 2011. Phosphorus removal from spiked
612 municipal wastewater using either electrochemical coagulation or chemical coagulation
613 as tertiary treatment. *Separation and Purification Technology* 95, 16-25.

614 Wang, J.-J., Liu, X., Ng, T.W., Xiao, J.-W., Chow, A.T., Wong, P.K., 2013. Disinfection
615 byproduct formation from chlorination of pure bacterial cells and pipeline biofilms. *Water*
616 *Research* 47 (8), 2701-2709.

617 White, G.C., 1992. Handbook of chlorination. 3rd ed., Van Nostrand Reinhold Co., 227.
618 New York.

619 Wilpert, A.V., 1957. Über die Analyse von Hypochlorit und Chlorit in einer Lösung.
620 *Fresenius' Zeitschrift für analytische Chemie* 155 (5), 378-378.

621 Yan, J.-F., White, R.E., Griffin, R.B., 1993. Parametric studies of the formation of
622 calcareous deposits on cathodically protected steel in seawater. *Journal of the*
623 *Electrochemical Society* 140 (5), 1275-1280.

624 Zaleschi, L., Sáez, C., Cañizares, P., Cretescu, I., Rodrigo, M.A., 2013. Electrochemical
625 coagulation of treated wastewaters for reuse. *Desalination and Water Treatment* 51 (16-
626 18), 3381-3388.

627 Zongo, I., Hamma Maiga, A., Wéthé, J., Valentin, G., Leclerc, J.P., Paternotte, G.,
628 Lapicque, F., 2009. Electrocoagulation for the treatment of textile wastewaters with Al

629 or Fe electrodes: Compared variations of COD levels, turbidity and absorbance. Journal
630 of Hazardous Materials 169 (1-3), 70-76.

631

632

633

634

635

636

637

638

639

640

641

642

643

644 **List of Figures**

645 **Figure 1.** Variation of the *E. coli* concentration (1.a) and chlorine species (1.b) with the
646 applied electric charge during the ED-EC process. ■ Cl-ClO⁻; ▲ Cl-ClO₃⁻; ● Cl-ClO₄⁻;
647 □ Cl-Chloramines. (Anode: BDD; Cathode: SS; Bipolar electrode: Iron; j: 6.70 A m⁻²; *E.*
648 *colio*: 22,000 CFU 100ml⁻¹; T: 25°C; pH: 8.05).

649 **Figure 2.** Variation of the turbidity and the iron concentration with the applied electric
650 charge during the ED-EC process. (Anode: BDD; Cathode: SS; Bipolar electrode: Iron;
651 j: 6.70 A m⁻²; *E. coli*: 22,000 CFU 100ml⁻¹; T: 25°C; pH: 8.05).

652 **Figure 3.** Variation of the *E. coli* with the applied electric charge at different current
653 densities during the ED-EC process of urban wastewater. ■ 1.90 A m⁻²; *E. coli*: 90,000

654 CFU 100 ml⁻¹; pH: 7.98; ▲ 4.13 A m⁻²; *E. coli*₀: 35,000 CFU 100 ml⁻¹; pH: 8.06; ● 6.70
655 A m⁻²; *E. coli*₀: 22,000 CFU 100 ml⁻¹; pH: 8.05; □ 9.38 A m⁻²; *E. coli*₀: 31,000 CFU 100
656 ml⁻¹; pH: 8.35. (Anode: BDD; Cathode: SS; Bipolar electrode: Iron; T: 25°C).

657 **Figure 4.** Evolution of chlorine species with the applied electric charge at different
658 current densities during the ED-EC process of urban wastewater. (a) Free chlorine. Black
659 points: Cl-ClO⁻; Grey points: Cl-ClO₃⁻; White points: Cl-ClO₄⁻. (b) Combined chlorine.
660 ■ 1.90 A m⁻²; ▲ 4.13 A m⁻²; ● 6.70 A m⁻²; ◆ 9.38 A m⁻². (Anode: BDD; Cathode: SS;
661 Bipolar electrode: Iron; T: 25°C).

662 **Figure 5.** Variation of the turbidity with the applied electric charge at different current
663 densities during the ED-EC process. ■ 1.90 A m⁻²; Turbidity₀: 13 NTU; pH: 7.98; ▲ 4.13
664 A m⁻²; Turbidity₀: 15 NTU; pH: 8.06; ● 6.70 A m⁻²; Turbidity₀: 14 NTU; pH: 8.05; □ 9.38
665 A m⁻²; Turbidity₀: 13 NTU; pH: 8.35. (Anode: BDD; Cathode: SS; Bipolar electrode:
666 Iron; T: 25°C).

667 **Figure 6.** Variation of the *E. coli* (black points) and the turbidity (white points) with the
668 applied electric charge during the ED-EC process of urban wastewater with different cell
669 configurations. ■□ C-A (j: 6.70 A m⁻²; *E. coli*₀: 22,000 CFU 100ml⁻¹; Turbidity₀: 14 NTU;
670 T: 25°C; pH: 8.05). ▲△ A-C (j: 6.76 A m⁻²; *E. coli*₀: 35,000 CFU 100ml⁻¹; Turbidity₀:
671 16 NTU; T: 25°C; pH: 8.35). (Anode: BDD; Cathode: SS; Bipolar electrode: Iron; T:
672 25°C).

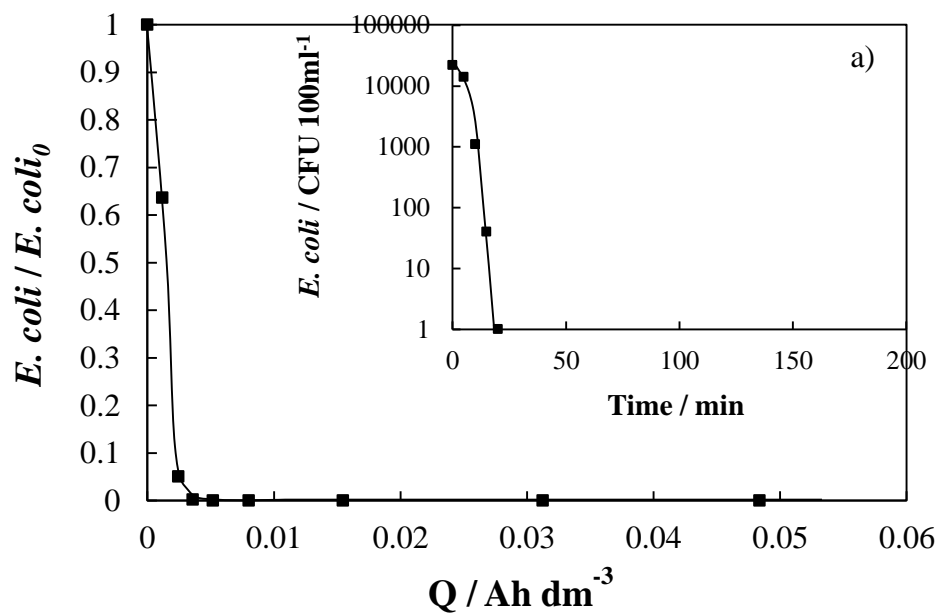
673 **Figure 7.** Removal of *E. coli* concentration (a) and the turbidity (b) at three different
674 applied electric charges and with different bipolar electrode materials. Black bars: iron
675 bipolar electrode (j: 6.70 A m⁻²; *E. coli*₀: 22,000 CFU 100ml⁻¹; Turbidity₀: 14 NTU; T:
676 25°C; pH: 8.05), hatched bars: aluminium bipolar electrode (j: 6.62 A m⁻²; *E. coli*₀: 25,000
677 CFU 100ml⁻¹; Turbidity₀: 8 NTU; T: 25°C; pH: 8.50). (Anode: BDD; Cathode: SS; T:
678 25°C).

679 **Figure 8.** Evolution of the metal concentration electrodisolved with the applied electric
 680 charge during the ED-EC process. (a) ■ Aluminium; j: 6.62 Am⁻² □ Iron; j: 6.70 Am⁻².
 681 (b) ■ Aluminium; j: 127.32 Am⁻² □ Iron; j: 116.59 Am⁻². (Anode: BDD; Cathode: SS; T:
 682 25°C).

683

684

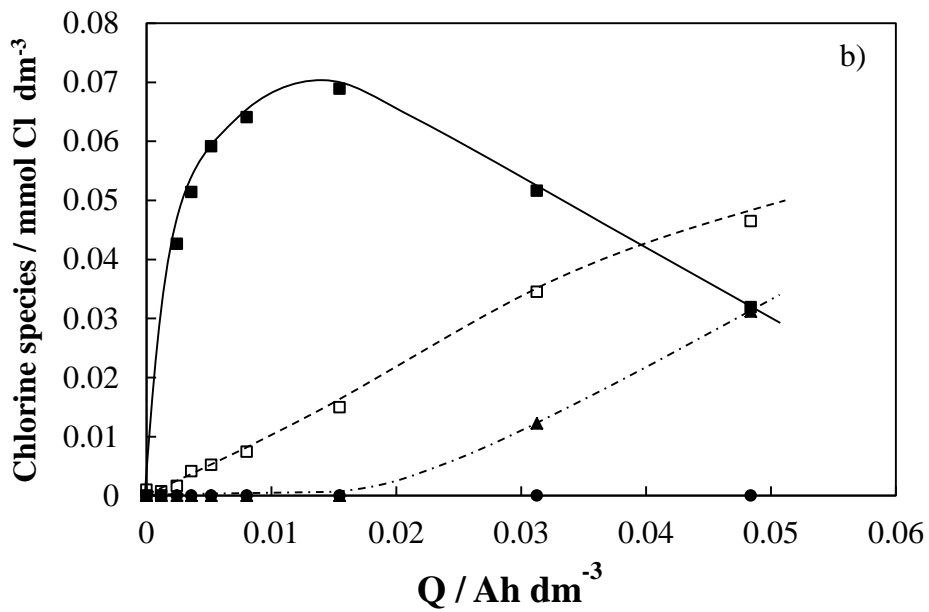
685



686

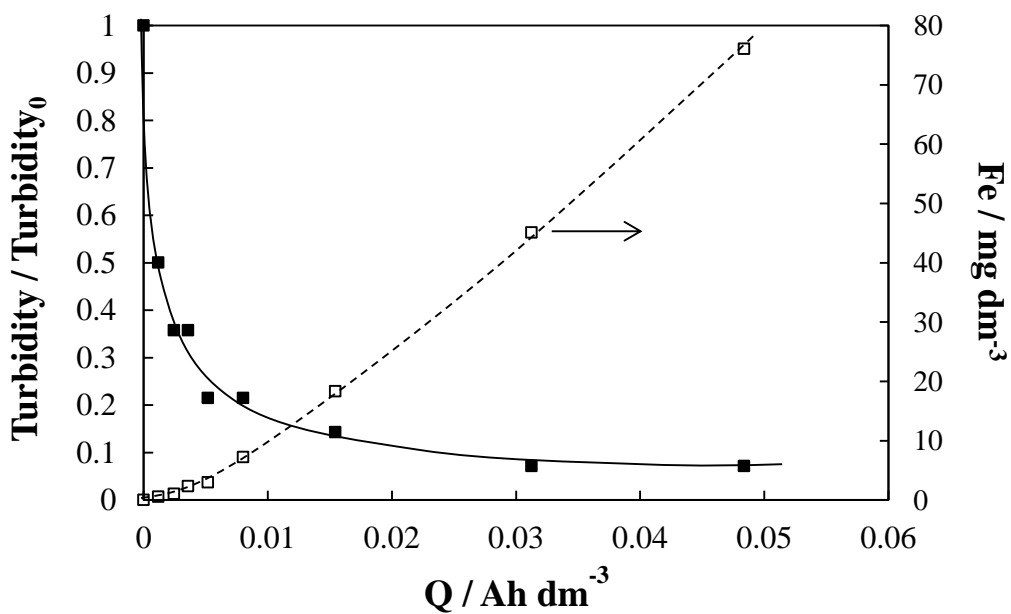
687

688



689
690
691
692
693
694
695
696
697
698
699

Figure 1



700
701
702
703
704
705

Figure 2

706
707
708
709
710
711
712
713
714
715
716
717
718

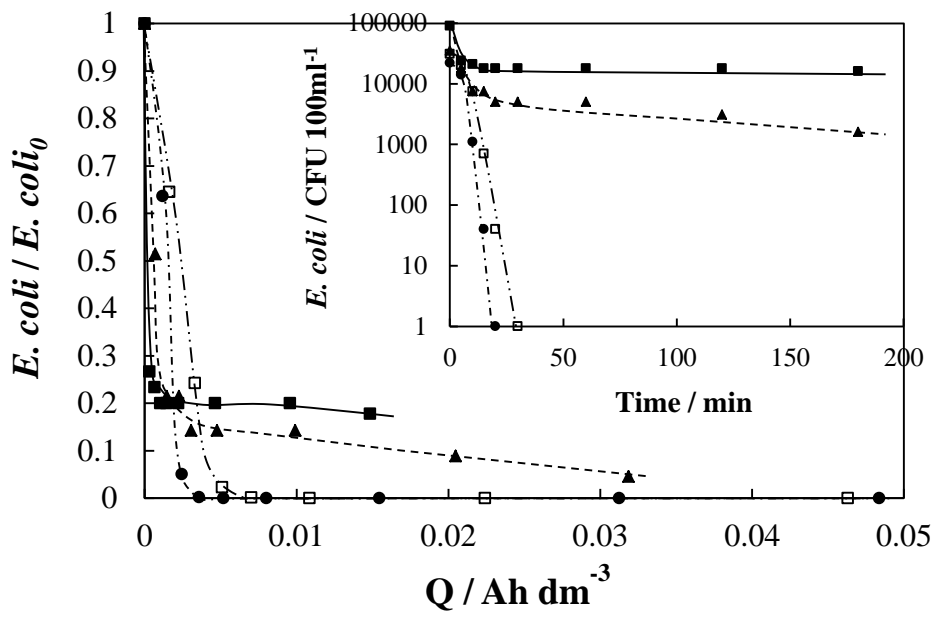
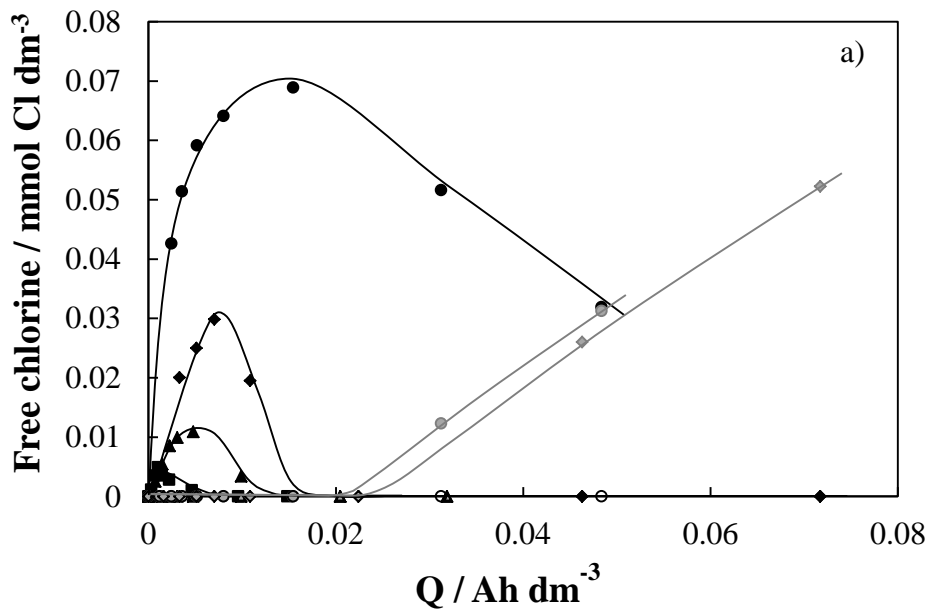


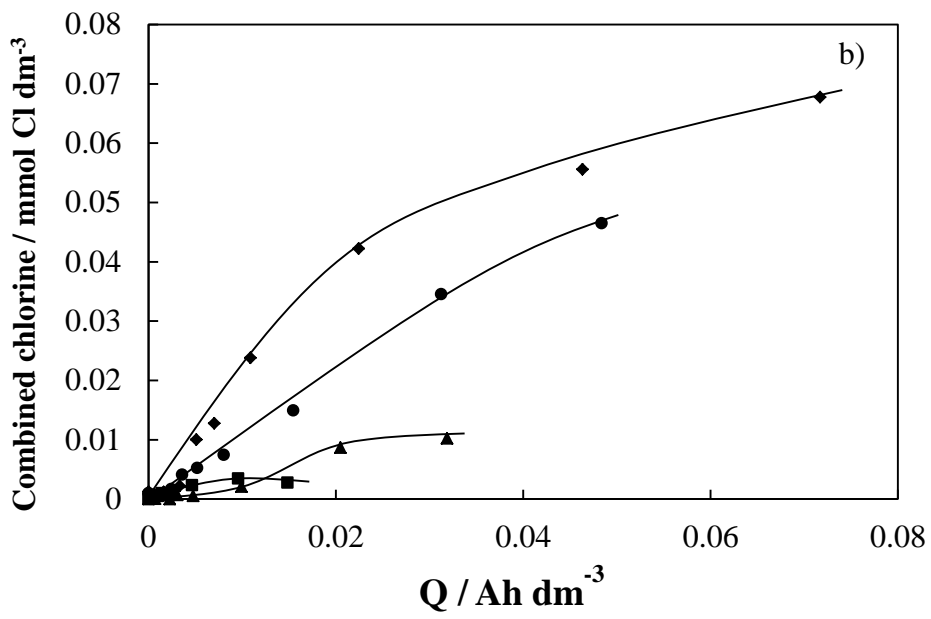
Figure 3

719
720
721
722
723
724
725
726
727
728
729
730
731
732
733
734
735
736
737
738
739

740



741
742
743
744



745
746
747
748
749
750
751
752
753
754
755
756

Figure 4

757

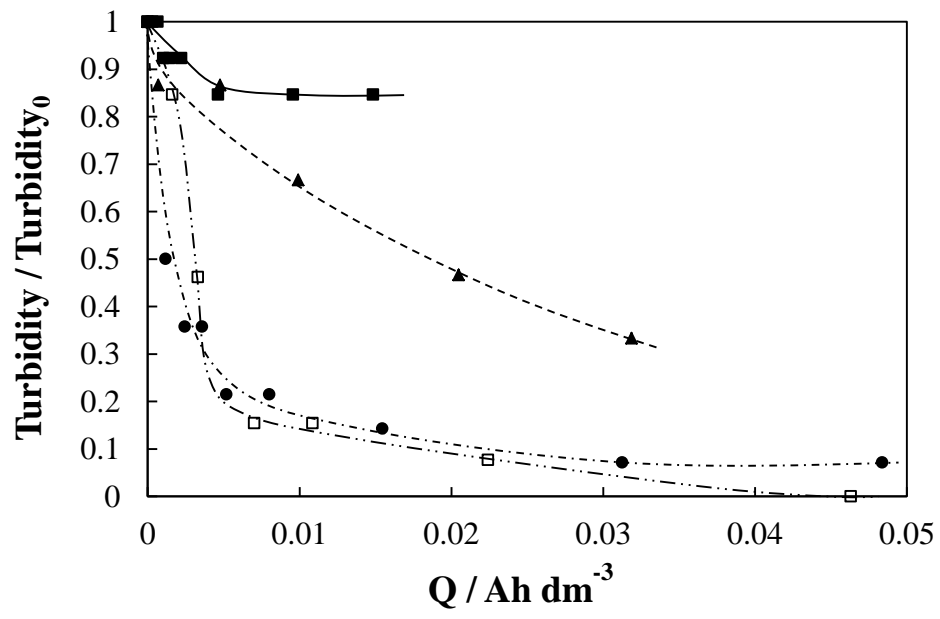


Figure 5

758
759
760
761
762
763
764
765
766
767
768
769
770
771
772
773
774

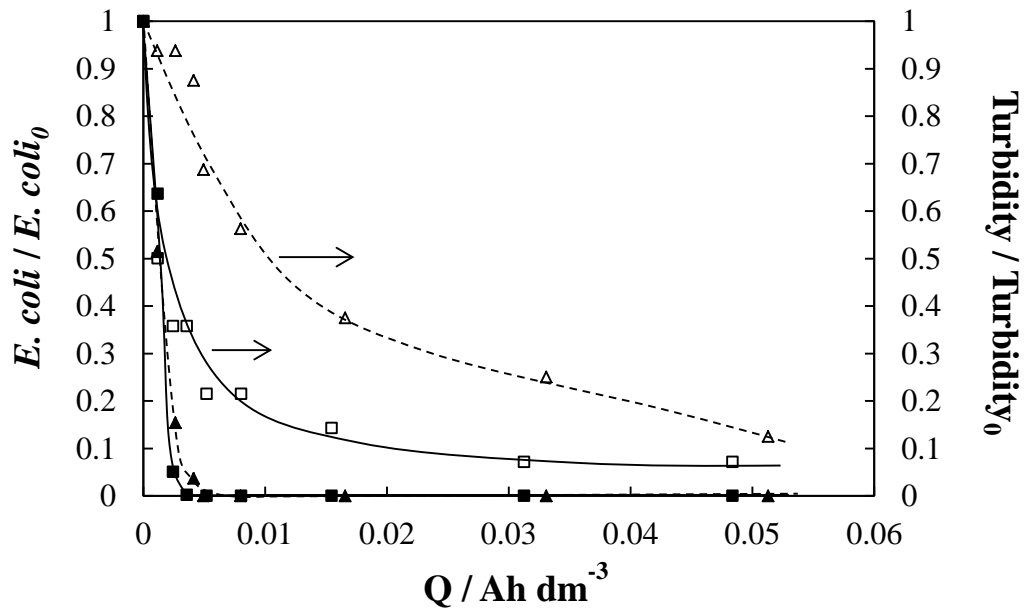
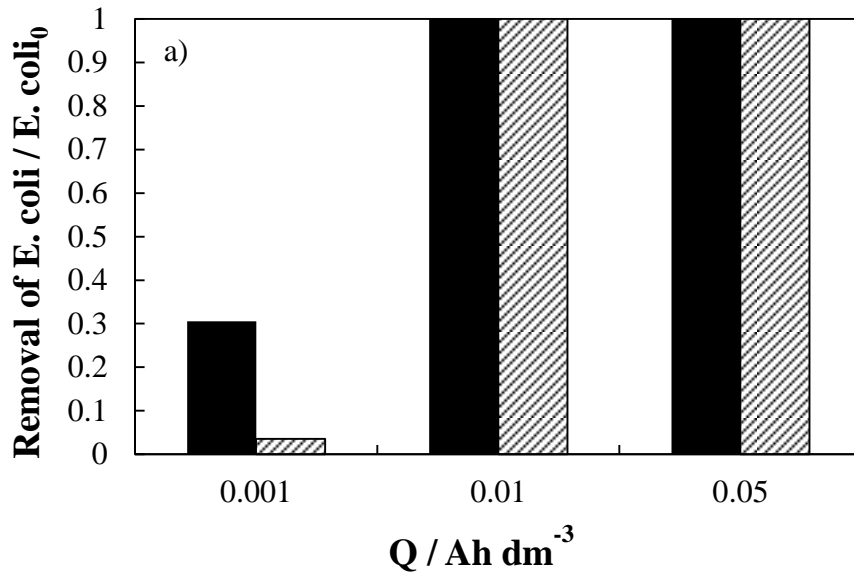
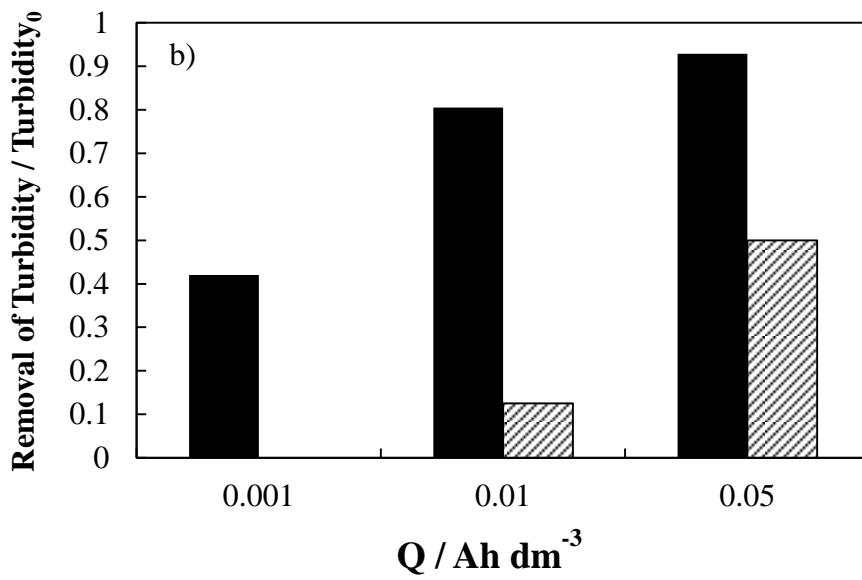


Figure 6

775
 776
 777
 778
 779
 780
 781
 782
 783
 784
 785
 786
 787
 788
 789
 790
 791
 792
 793
 794
 795
 796
 797

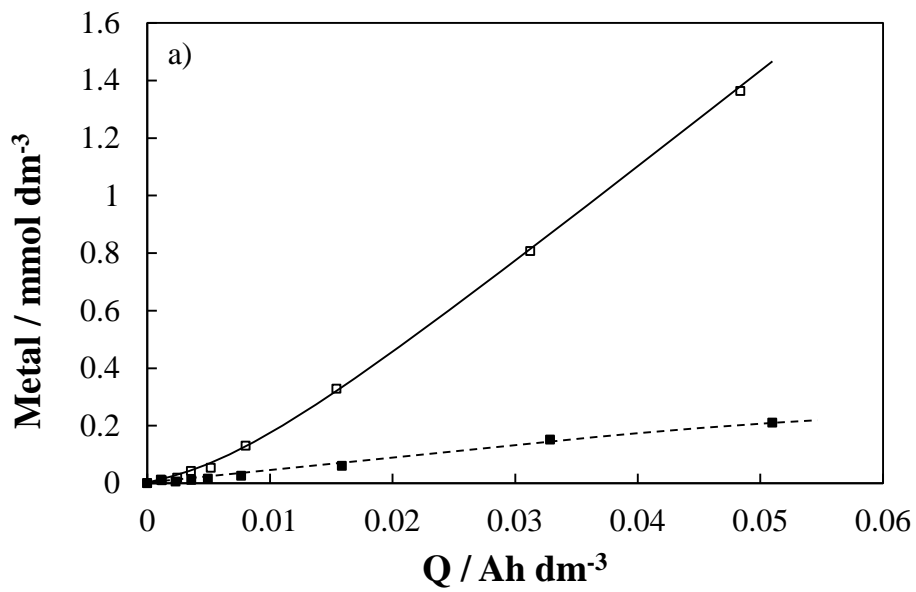


798
799
800
801

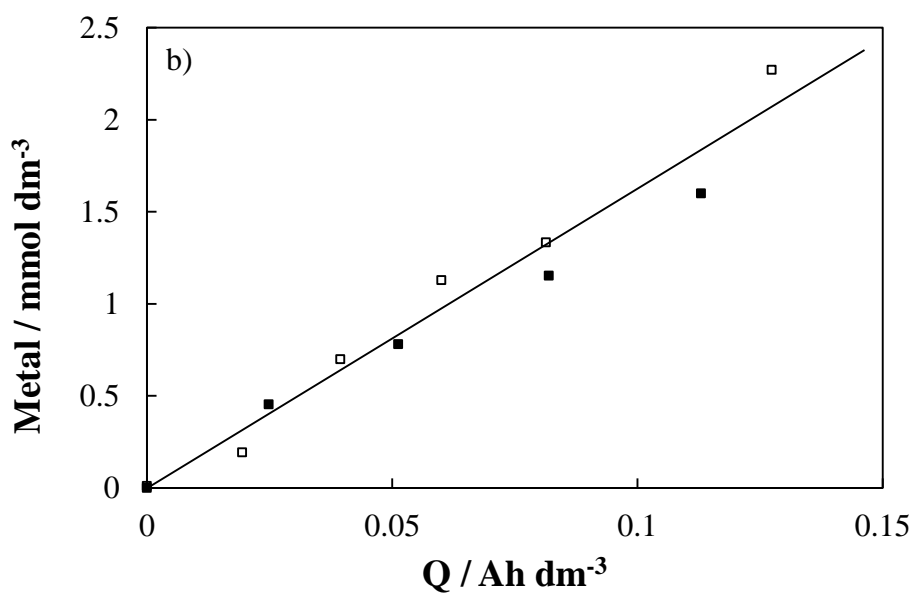


802
803
804
805
806
807
808
809
810
811

Figure 7



812
813
814
815
816
817



818
819
820
821
822
823
824
825
826
827
828
829

Figure 8

830 **List of Tables**831 **Table 1.** Average composition of target wastewater.

Parameter	Value
Chloride (mg dm ⁻³)	204.850
Nitrate (mg dm ⁻³)	23.740
Sulphate (mg dm ⁻³)	334.595
Ammonium (mg dm ⁻³)	43.434
Iron (mg dm ⁻³)	n. d.
Aluminium (mg dm ⁻³)	n. d.
Turbidity (NTU)	13-15
TSS (mg dm ⁻³)	7-10
TOC (mg dm ⁻³)	25
<i>E. coli</i> (CFU 100ml ⁻¹)	22000-90000
n. d. – non detectable TSS – Total suspended solids TOC – Total organic carbon	

832

833